

# Transient Response of a Projectile in Gun Launch Simulation Using Lagrangian and ALE Methods<sup>1</sup>

Ala Tabiei <sup>2</sup>

*Department of Aerospace Engineering & Engineering Mechanics  
University of Cincinnati, Cincinnati, OH 45221-0070*

Mostafiz R. Chowdhury

*U.S. Army Research Laboratory  
2800 Powder Mill Rd  
Adelphi, MD 20783-1145*

## ABSTRACT

*This paper describes the usefulness of Lagrangian and arbitrary Lagrangian/Eulerian (ALE) methods in simulating the gun launch dynamics of a generic artillery component subjected to launch simulation in an air gun test. Lagrangian and ALE methods are used to simulate the impact mitigation environment in which the kinetic energy of a projectile is absorbed by the crushing of an aluminum honeycomb mitigator. Issues related to the effectiveness of these methods in simulating a high degree of distortion of Aluminum honeycomb mitigator with the commonly used material models (metallic honeycomb and crushable foam) are discussed. Both computational methods lead to the same prediction for the deceleration of the test projectile and are able to simulate the behavior of the projectile. Good agreement between the test results and the predicted projectile response is achieved via the presented models and the methods employed.*

**KEYWORDS:** Lagrangian, ALE method, honeycomb mitigator, air gun launch simulation

<sup>1</sup>Approved for public release; distribution is unlimited.

<sup>2</sup>Author to whom correspondence should be addressed.

## INTRODUCTION

An air gun test provides an efficient and effective launch simulation platform in which the shock phenomena in a real gun test are replicated in a controlled environment. The primary focus of such an air gun mitigation test is to simulate a transient shock environment that the test projectile is anticipated to encounter in an actual field test. Proper simulation of the gun launch environment via an air gun test requires a thorough understanding of the dynamics of the physical energy-absorbing interfacing components that regulate its shock environment. An analytical model in this regard could play a vital role in facilitating design and preparation of an effective air gun test. The ability to numerically simulate the dynamic response of the test projectile will allow the physical operating parameters of the air gun test environment to be tuned to achieve the specific dynamic profile for which the projectile has been tested. This methodology requires the development of a predictive model of responses of the test projectile. This paper presents the development of a finite-element (FE) model to simulate the dynamic impact response of a generic artillery component mounted on a given projectile during gun launch simulation in an air gun test.

Several LS-DYNA models of a generic test article fired in a 101.6-mm (4-in.) air gun chamber are developed in this study. Control test data for a test item mounted on a projectile are used for model validation and correlation. Analytical simulation of the air gun launch environment requires the modeling of an event in which the test object mounted on a projectile is launched and decelerated when it crushes an aluminum (Al) honeycomb mitigator in the recovery chamber. As a secondary energy-absorbing device, a momentum exchange mass (MEM) is used at the retrieving end. Two formulations are used in the simulations using explicit finite-difference methods. These included the Lagrangian and the arbitrary Lagrangian/Eulerian (ALE) formulations. Benson [1] reviews the basic explicit methods for solving transient, large deformation problems in solid mechanics.

During the crush simulation, the Al honeycomb mitigator undergoes significant deformation that could render a severely unstable Lagrangian simulation. For this reason, an ALE simulation is also considered. The Eulerian method is more suitable for problems involved in severe mesh distortion. The Lagrangian method, on the other hand, is limited in how much an element can deform. The Lagrangian method is easy to set up and visualize since the material point moves with the mesh. However, the Eulerian method is more difficult to set up and the mesh is stationary so that material points are advected from one element to the next. The Eulerian method allows new free surfaces to be created in a natural manner. An ALE method is a combination of Lagrangian and Eulerian formulations in which the parts that endure very large deformation such as those involving material flow are modeled with the Eulerian approach.

Two material formulations are used for simulating the Al honeycomb mitigator behavior with the Lagrangian method. These included honeycomb and crushable foam material models. The honeycomb material model simulates an anisotropic crushable behavior of a fully uncoupled system. The crushable foam material model, on the other hand, simulates an isotropic crushable behavior of a coupled system. This isotropic foam model crushes one dimensionally with a Poisson's ratio that is essentially zero. Most of the Al honeycomb material in the air gun simulation is crushed axially. Therefore, the crushable foam model is considered to be appropriate for simulating crushing behavior of an Al mitigator in the air gun test. The honeycomb material model formulation requires stress versus logarithmic strain relationship.

Stress versus volumetric strain relationship is used to formulate the crushable foam material model. Only the crushable foam material model is used in the ALE method. The effectiveness of these two material models, along with the applicability of Lagrangian and ALE methods, are described next.

## 2. AIR GUN TEST DESCRIPTIONS

A schematic diagram for a typical air gun test setup is shown in Figure 1. The test setup consists of a stationary gun barrel, a projectile, and a dual energy-absorbing mechanism consisting of a mitigator and a MEM positioned at the recovery end. In a typical air gun mitigation test, the projectile carrying the artillery components to be tested is launched to impact an Al honeycomb mitigator at the recovery chamber. Upon impact with the mitigator, the kinetic energy of the projectile is lessened as the mitigator crushes. The crushed mitigator in turn exchanges its momentum with a MEM, a secondary energy-absorbing device, abutting its rear end.

A pre-shot arrangement of the dual energy-absorbing devices in an air gun retrieving chamber is shown in Figure 2. As seen in the figure, the mitigator is stationed inside the split catch tube at the start of the test. Four 12.7-mm (0.5-in.) diameter, 4340 steel tie rods (two each side of the isle; see Figure 2) are used to fasten the top half of the split catch tube with the stationary bottom half shown in the figure. The striking end of the 0.6087-gm/cm<sup>3</sup> (38-pcf) Al honeycomb mitigator was fashioned to form two sharp wedges. The 7075-T6 Al mitigator was 256.54 mm (10.1 in.) long, including a wedge depth of 38.1 mm (1.5 in.), 98.30 mm (3.87 in.) in diameter, and weighed about 1,110 gm. With two such wedges at the striking end, the mitigator tends to crush evenly across its face. The length of the wedges also determines the projectile's deceleration profile during the impact. The MEM at the recovery end weighed about 31,300 gm. A post-shot relative position for the physical apparatus is shown in Figure 3. As seen in this figure, upon hitting its target, the projectile remains trapped in the catch tube, the mitigator crushes, and the MEM displaces. An enlarged view of the crushed mitigator and the undeformed test projectile is shown in Figure 4. A post-test configuration of the mitigator shows that the striking end of the mitigator solidifies more than its remote end.

A test projectile consisting of a rectangular Al plate (101.0 mm [4.9 in.] x 76.2 mm [3 in.] x 12.7 mm [0.5 in.]) mounted on the top of an on-board recorder (OBR) case (152.4 mm [6 in.] in length, 101.09 mm [3.98 in.] in outer diameter with a thickness of 12.7 mm [0.5 in.]) was especially prepared for FE verification. The projectile including the OBR carrier and a rectangular plate mounted on its top weighed about 3,250 gm. In this test projectile, OBR records the data and the plate is the test item representing a simulated projectile component that could be used in an actual air gun test.

Figure 5 shows the test projectile and the instrument locations for which the data were recorded via an on-board 12-bit, 4-channel high shock analog recorder placed inside the OBR case. Two accelerometers and two strain gauges were mounted on the test item. The analog recorder was shock isolated inside the canister by the suspension of the device over glass beads and the canister being densely packed once the top mount had been assembled. An isolated packaging arrangement was needed to ensure survival of the OBR.

### 3. MATERIAL MODELS

One of the most difficult aspects of this investigation was to define the material properties that would represent the physical behavior of the Al honeycomb mitigator used in the air gun test. In this investigation, no test was conducted for characterizing mitigator properties. Therefore, the authors had to depend on the data available in the open literature. The crush test results available in reference [2] were used to construct the material model. As shown in Figure 6, three distinct features characterize the honeycomb mitigator's load-carrying behavior. These features included a linear elastic tendency until initial crushing, typical volumetric crush, and final phase of hardening to full compaction. Almost all energy absorption is done in the volumetric crush zone. Initial spikes at the end of linear behavior are typical in the Al honeycomb resistance profile, which can be eliminated by the crushing of the mitigator's striking edge. The fluctuation of strength during volumetric crushing, as seen in the figure, may have resulted from instability because of buckling of honeycomb cells.

The two material models considered here are honeycomb and crushable foam material formulations. The formulations of the two material models are described next.

#### 3.1 Honeycomb Material Model

This material model is suited to model metallic honeycomb [3,4,5]. The behavior before compaction is orthotropic where the components of the stress tensor are uncoupled, i.e., a component of strain will generate resistance in the local a-direction with no coupling to the local b and c directions. The elastic moduli ( $E$ ) vary from their initial values to the fully compacted values linearly with the relative volume:

$$\begin{aligned} E_{aa} &= E_{aau} + \beta(E - E_{aau}) & G_{ab} &= G_{abu} + \beta(G - G_{abu}) \\ E_{bb} &= E_{bbu} + \beta(E - E_{bbu}) & G_{bc} &= G_{bcu} + \beta(G - G_{bcu}) \\ E_{cc} &= E_{ccu} + \beta(E - E_{ccu}) & G_{ca} &= G_{cau} + \beta(G - G_{cau}) \end{aligned}$$

in which

$$\beta = \max \left[ \min \left( \frac{1-V}{1-V_f}, 1 \right), 0 \right]$$

and  $G$  is the elastic shear modulus for the fully compacted honeycomb material:

$$G = \frac{E}{2(1+\nu)}$$

The relative volume,  $V$ , is defined as the ratio of the current volume over the initial volume, and typically,  $V = 1$  at the beginning of a calculation.

At the beginning of the stress revision, each element's stresses and strain rates are transformed into the local element coordinate system. For the uncompacted material, the stress components are revised by the elastic interpolated moduli according to the following:

$$\begin{aligned}\sigma_{aa}^{n+1,trial} &= \sigma_{aa}^n + E_{aa} \Delta \varepsilon_{aa} & \sigma_{ab}^{n+1,trial} &= \sigma_{ab}^n + E_{ab} \Delta \varepsilon_{ab} \\ \sigma_{bb}^{n+1,trial} &= \sigma_{bb}^n + E_{bb} \Delta \varepsilon_{bb} & \sigma_{bc}^{n+1,trial} &= \sigma_{bc}^n + E_{bc} \Delta \varepsilon_{bc} \\ \sigma_{cc}^{n+1,trial} &= \sigma_{cc}^n + E_{cc} \Delta \varepsilon_{cc} & \sigma_{ca}^{n+1,trial} &= \sigma_{ca}^n + E_{ca} \Delta \varepsilon_{ca}\end{aligned}$$

We then independently check each component of the revised stresses to ensure that they do not exceed the permissible values determined from the load curves; e.g., if

$$|\sigma_{ij}^{n+1,trial}| > \lambda \sigma_{ij}(\varepsilon_{ij})$$

then

$$\sigma_{ij}^{n+1} = \sigma_{ij}(\varepsilon_{ij}) \frac{\lambda \sigma_{ij}^{n+1,trial}}{|\sigma_{ij}^{n+1,trial}|}$$

The components of  $\sigma_{ij}(\varepsilon_{ij})$  are defined by load curves.

The material model requires the stress versus logarithmic strain input for material characterization [6]. The relation between the engineering strain,  $e$  and the logarithmic strain,  $\varepsilon$

is given by  $\varepsilon = \ln(1 + e) = \ln(\frac{L}{L_o})$

in which the engineering strain,  $e$ , is defined by the equation  $e = \frac{L - L_o}{L_o} = \frac{L}{L_o} - 1 = \frac{\Delta L}{L_o}$ .

For instance, if the efficiency of the honeycomb material is 90%, the material final length is only 10% of its initial length. The logarithmic strain in this case is  $\varepsilon = \left| \ln\left(\frac{0.1}{1.0}\right) \right| = 2.3026$ .

### 3.2 Crushable Foam Material Model

This material model is suited for modeling crushable foam [3,4,5]. This isotropic foam model crushes one dimensionally with a Poisson's ratio that is essentially zero. In the implementation, we assume that Young's modulus is constant and revise the stress, assuming elastic behavior.

$$\sigma_{ij}^{n+1,trial} = \sigma_{ij}^n + E \dot{\varepsilon}_{ij}^{n+1/2} \Delta t^{n+1/2}$$

The magnitudes of the principal values  $\sigma_i^{trial}$ ,  $i = 1, 3$  are then checked to see if the yield stress  $\sigma_y$  is exceeded; if so, they are scaled back to the yield surface so that, if

$$\sigma_y < |\sigma_i^{trial}|$$

then

$$\sigma_{ij}^{n+1} = \sigma_y \frac{\sigma_i^{trial}}{|\sigma_i^{trial}|}$$

After the principal values are scaled, the stress tensor is transformed back into the global system.

The material model requires the stress versus volumetric strain relationship [6]. The volumetric strain  $\varepsilon_v$  is defined as  $\varepsilon_v = 1 - \frac{V}{V_o} = 1 - \frac{AL}{A_o L_o}$ .

Since we can assume that the crushable foam is crushed under a very small Poisson's ratio, the initial cross-sectional area is the same as the final one. Therefore, in this case the volumetric strain can be simplified as  $\varepsilon_v = 1 - \frac{L}{L_o}$ .

### 3.3. Material Parameters

Parameters of interest for the material model include crush strength, crush efficiency (volumetric strain that initiates the hardening), hardening modulus, and strain rate enhancement attributable to increase in impact velocity. In this investigation, a stress scale factor (relative increase in strength because of impact velocity) suggested by Bitzer [7], which ranges from 1.2 to 1.5, is used because of the unavailability of high strain rate-dependent experimental data. In order to verify the validity of the materials models, an FE model was developed to simulate the compression test reported in literature [2]. The displacement control is used in the simulation. The simulated stress-strain curves for 90% and 64% compaction are compared in Figure 6 for both material models. This figure clearly identifies three distinct features in load-carrying behavior of honeycomb materials. These features included linear elastic tendency until initial crushing, typical volumetric crush, and final phase of hardening to full compaction. Almost all energy absorption is done in the volumetric crush zone. Initial spikes at the end of linear behavior are typical in Al honeycomb resistance profile, which can be eliminated by the crushing of the mitigator's striking edge.

The mean values and the overall trends in the simulated curve closely match the test data presented by Lu and Hutchinson [2]. A 90% efficiency means that the final length is only 10% of its initial length. Predicted crushing strain, thus for 90% efficiency (~2.5 mm/mm) is greater than the 64% case (~1 mm/mm) as indicated in Figure 6. A simulation is also performed for the static and rate sensitive cases. Results indicate that the rate-sensitive stress is about two times the static stress [8]. This simulation testifies to the effectiveness of the proposed material models in simulating the mean load-displacement relationship of the Al honeycomb mitigator. This material model, however, disregards the strength fluctuation during volumetric crush as evidenced in the physical tests data shown in reference [2].

## 4. THE FINITE ELEMENT MODELS

### 4.1. Lagrangian Model

The FE model of the Lagrangian test setup is depicted in Figure 7. The model consists of the catch tube (the wired mesh), the OBR (the brown mesh), the instrumented plate (the dark blue mesh), the MEM, (the yellow mesh), and four beam elements that represented the bolts connecting the two halves of the catch tubes. Upon modeling the OBR, no inner filler materials including the recording devices and the glass beads, were included in the FE model. We

simulated the total mass of the instrumented OBR in the FE model by adjusting the density of the OBR canister. The analytical simulation of the impact starts with an initial input velocity for the projectile from the position shown in the figure.

The FE model consists of 118,842 nodes and 123,164 elements. There are 14,744 shell elements, 108,416 solid elements, and 4 beam elements in the model. Several contact surfaces are defined in this model. A contact surface is defined between the OBR and the mitigator, the OBR and the catch tube, the mitigator and the catch tube, and the mitigator and the MEM. The segment-based contact is used in this case, which proved to be more stable. Both material models, honeycomb and crushable foam, are used in this model.

#### ***4.2. ALE Model***

Since it is difficult to simulate very large deformation in the Lagrangian method easily, the ALE method is employed. The Lagrangian method requires significant expertise in the modeling of severe deformation. The ALE method, on the other hand, is more stable for such problems. The mesh model reported in this paper consisted of 69,578 node and 65,724 elements. There are 4,440 shell elements, 61,280 solid elements, and 4 beam elements in the model. The ALE FE model consists of the catch tube, the OBR (glass beads are not modeled as in Lagrangian case), the instrumented plate, and the MEM that is similar to the Lagrangian model. The mitigator, however, is modeled differently here. The mitigator is modeled with solid element formulation No. 12 in LS-DYNA. This element formulation is ALE plus void. The mesh in this part does not distort, which is the case with Eulerian description of motion. The mitigator is surrounded by void elements. The void element is there for the possibility of the mitigator material flow. Upon deformation, the mitigator material can flow outside of the mitigator mesh. Once this happens, the mitigator material can flow into the void elements. The solid elements of the mitigator and void have node-to-node correspondence at the boundaries. Figure 8 depicts a section cut through the middle of the mesh. The blue mesh represents the mitigator honeycomb and the red mesh is the surrounding void.

The integration time step in an ALE simulation is smaller than a Lagrangian simulation for the same mesh size. The explicit time integration time step in the Lagrangian method, in general, is a function of the smallest element's characteristic length and material properties. In the ALE method, in addition to the above, it is also a function of mesh velocity. Therefore, the integration time step in the ALE method is smaller than the Lagrangian method.

## **5. SIMULATION RESULTS**

The simulations are performed on a 1.7-MHz laptop computer and also independently on an Army Research Laboratory Major Shared Resource Center's SGI Origin 2000 system. The impact event is about 2 milliseconds (ms). The contact of the OBR with the mitigator is about 1 ms only. The CPU time with the laptop for the Lagrangian simulation is about 4 hours. The Eulerian simulation takes about 16 hours to completion even though the number of elements is about half those of the Lagrangian simulation. The impact velocity in both models is taken as 83,566 mm/sec (3,290 in./sec.) We obtained the initial velocity by double integrating the recorded accelerometer data from the actual test shot. The three fundamental units used here are millimeter (mm), second (sec), and metric ton for the length, time, and mass, respectively. Results of the two simulations are presented next.

### 5.1. Lagrangian Simulations

Results of the simulations using both material models are presented next.

#### 5.1.1 Honeycomb Material Model

The strain rate effect must be included in such a simulation since the material exhibits strain rate sensitivity. However, since experimental data for the used honeycomb material under high strain rate are not available, the stresses are scaled by a multiplier. The range of stress scale factor used is between 1.2 and 1.5 for this material model [7].

The honeycomb material reported in reference [2] has an efficiency of 64 to 90%. The 64% efficiency (or compaction) predicted a stiffer response than the 90% compaction. Figure 9 shows the difference in predictions of the two efficiencies.

Figure 10 shows the impacted geometry and a view of the impacted geometry of the air gun launch simulation. Figure 11 depicts the energy balance as predicted by the simulation. One can see that the energy is conserved in this simulation, which is an indication of numerical stability of the model. The hourglass energy and contact energy (not shown here) are much smaller than the internal energy as desired in a stable impact simulation.

#### 5.1.2 Crushable Foam Material Model

The CPU time for the simulation with this material model is about the same as for the honeycomb material model discussed before. The crushed mitigator is shown in Figure 13. A stress scale factor of 1.5 is used to account for the strain rate sensitivity. The qualitative difference between the simulations with honeycomb and crushable foam models was insignificant. Figure 14 shows the filtered acceleration of the top of the OBR for both material models. The magnitude of the acceleration for the two materials is about the same. However, there is some difference in the duration of the pulse. This difference is attributed to the differences in the formulation of the two material models. The honeycomb model is an orthotropic material, which assumes that stress components are fully decoupled. Straining of the material in the local material axis in one direction causes stress in that direction only. However, the crushable foam is an isotropic material model and the stress components are not decoupled.

### 5.2 ALE Simulation

The mesh is fixed in an ALE simulation. In this situation, one can look at the volume fraction of the material. The volume fraction is equal to 1 when the element is filled with the material. A volume fraction of less than 1 means that only part of the element is filled with the material. The volume fraction of the mitigator material at the end of the simulation is depicted in Figure 15. One can observe that the Eulerian mesh has not moved; however, the material has passed from one element to next, indicating material flow and deformation.

A comparison of the prediction of the acceleration of the top of the OBR via the Lagrangian and ALE methods is shown in Figure 16. These data are filtered with a low pass filter with a cut-off frequency of 2500 Hz. A small difference is observed in the magnitude of the peak acceleration.

This difference, however, can be neglected and assumed to be the numerical error difference between the two methods.

## 6. MODEL VALIDATION: SIMULATION VERSUS EXPERIMENT

The simulation results are compared with experiments qualitatively and quantitatively. Qualitatively, the deformation of the mitigator looks the same in the simulation and experiment. The experimental final crushed length of the mitigator is reported as 210.0 mm (8.27 in.). The simulated final crushed length of the mitigator is predicted to be 226.0 mm (8.90 in.) —A difference of about 7% from the actual crushed length.

The quantitative validation consists of comparing the acceleration data from simulation and experiment for the locations shown in Figure 5. The locations of nodes for which the data were extracted are at the same locality as in the test setup.

For comparison purposes, the simulation results and the experimental results are filtered with low pass cut-off frequencies of 7000 Hz and 2500 Hz, respectively. The simulations and the experiment's acceleration of the top of the OBR for both filtrations are shown in Figures 17 and 18. Figure 17 shows a relatively good agreement between the predicted and test acceleration responses with the honeycomb material model when a stress scaled factor of 1.5 was used in the analysis. A higher stress scale factor (1.5 instead of 1.2) has significantly attenuated the free vibration, as indicated in Figure 17. Good prediction is observed from the simulation as compared to experiment, particularly for the 2500-Hz cut-off frequency. Figure 18 compares several runs for the simulation. Two predictions are presented for the honeycomb material model with two different stress factors (1.2 and 1.5). One can observe that when the stress is scaled by 1.2, the peak acceleration is under-predicted. When the stress is scaled by 1.5, the peak acceleration is over-predicted. Figure 18 also shows the prediction of acceleration with the crushable foam material model. In this case, the stress is also scaled by 1.5.

## 7. CONCLUSIONS

Lagrangian and ALE methods are developed to simulate the air gun launch environment in which a test object mounted on a projectile is fired through the air gun and decelerated by the crushing of an Al honeycomb mitigator which impacts the MEM before being stopped at the retrieving end. The Lagrangian method is simpler to set up, post process, and requires less computational time. However, it requires significant expertise in the FE model to make the simulation numerically stable. This is because of the significant large deformation of the mitigator. On the other hand, the ALE method is more difficult to set up, post process, and requires much more CPU time. However, the ALE simulation is more suitable for very large deformation problems such as those involving material flow. Both computational methods lead to the same prediction for the acceleration of the OBR.

Both material models, honeycomb and crushable foam, lead to reasonable predictions and are able to simulate the behavior of the mitigator. The strain rate sensitivity must be accounted for in these simulations. If no strain rate effect is included, the peak acceleration of the OBR is under predicted. In the presented simulation, instead of activating the rate effect in the material models,

the stress is scaled by values between 1.2 and 1.5. This will have the same effect as if the rate effect were activated in the material model.

Good prediction of the period and peak acceleration of the OBR is achieved with the presented models and the methods employed. A similar FE modeling technique can be used for such problems with confidence that the code will aid in the prediction of the proper response of any instrument mounted on the OBR.

### **ACKNOWLEDGMENTS**

The analytical work presented here was accomplished under a contract (TCN: 02-125) with the Scientific Services Program (STAS) of U.S. Army Research Office (ARO), Research Triangle Park, North Carolina. We greatly appreciate the services of ARO in facilitating the contract and the support of U.S. Army Research Laboratory in allowing us to publish the document.

### **REFERENCES**

- [1] D.J. Benson (1991). "Computational Methods in Lagrangian and Eulerian hydrocodes", Computer Methods in Applied Mechanics and Engineering, Vol 99, pp. 235-394.
- [2] W. Lu, and T. Hinnerichs, (2001). "Crush of High Density Aluminum Honeycombs", Proceedings of the International Mechanical Engineering Congress and Exposition, Nov 11-16.
- [3] J. Hallquist, (1998). 'LS-DYNA Theoretical Manual', LSTC, Livermore, CA.
- [4] J. Hallquist, (1998). 'LS-DYNA Users Manual, Vol. 1', LSTC, Livermore, CA.
- [5] J. Hallquist, (1998). 'LS-DYNA Users Manual, Vol. 2', LSTC, Livermore, CA.
- [6] A. Tabiei, (1999-2002). "Advance LS-DYNA Lecture Notes", Cincinnati, OH.
- [7] T. Bitzer, (1997). Honeycomb Technology, Champman & Hall, London, UK.
- [8] M.R. Chowdhury, and A. Tabiei, (2003). Development of An Air Gun Simulation Model Using LS-DYNA, Final Report, TCN 02-125, U.S. Army Research Office, RTP, NC

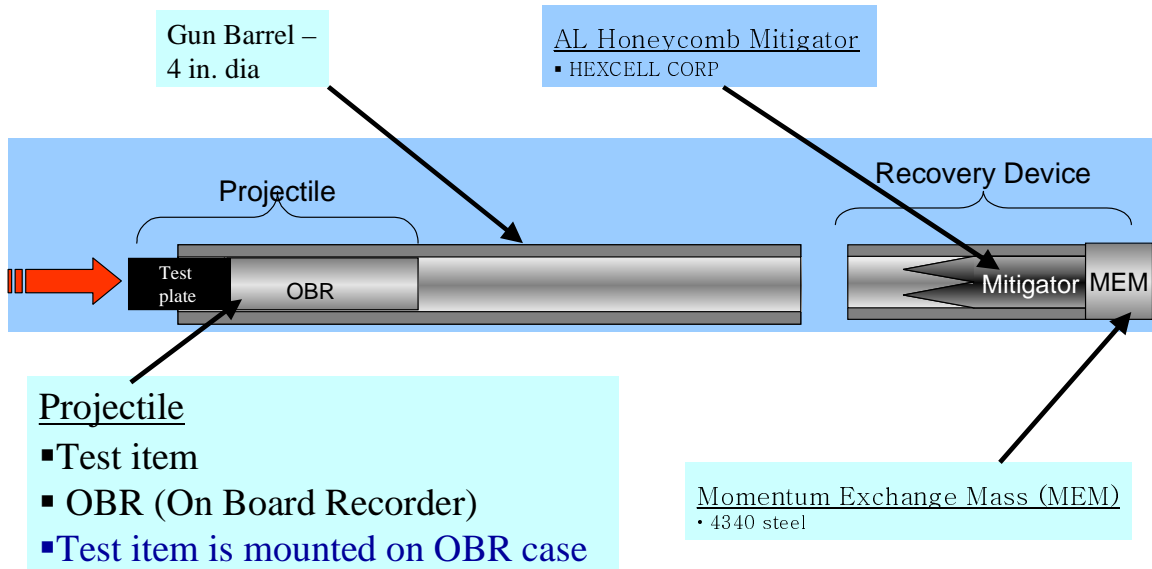


Figure 1. Schematic of an air gun test setup.

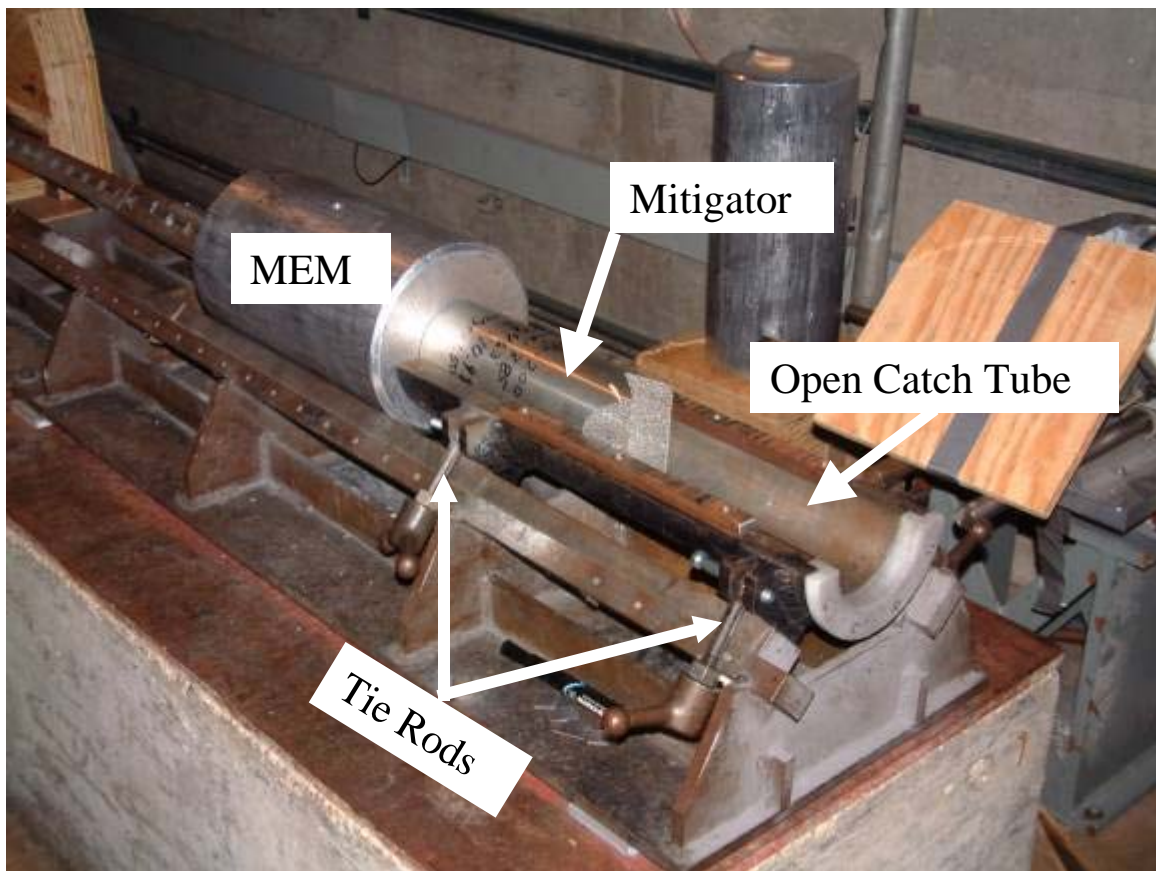


Figure 2. A pre-shot arrangement in the 4-inch air gun test.

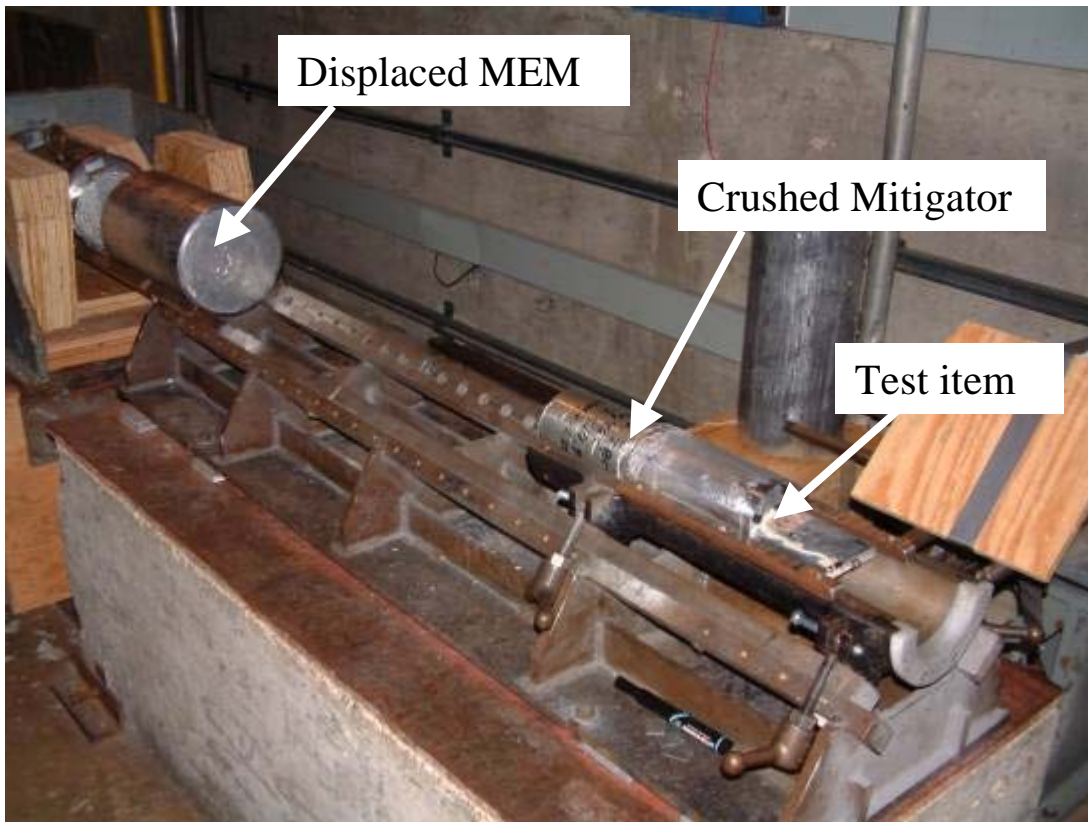


Figure 3. A post-shot configuration of interacting components in a 4-inch air gun test.

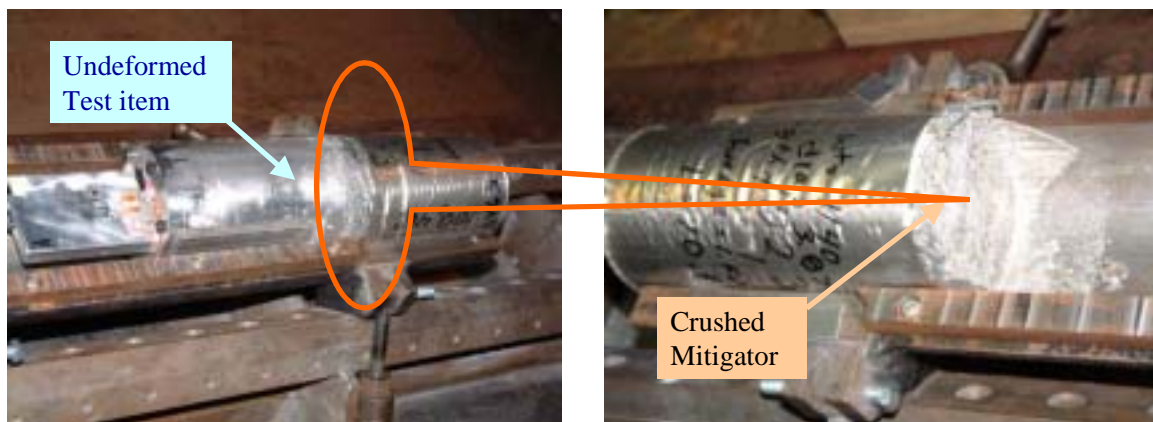


Figure 4. A post-shot view of an Al crushed mitigator.

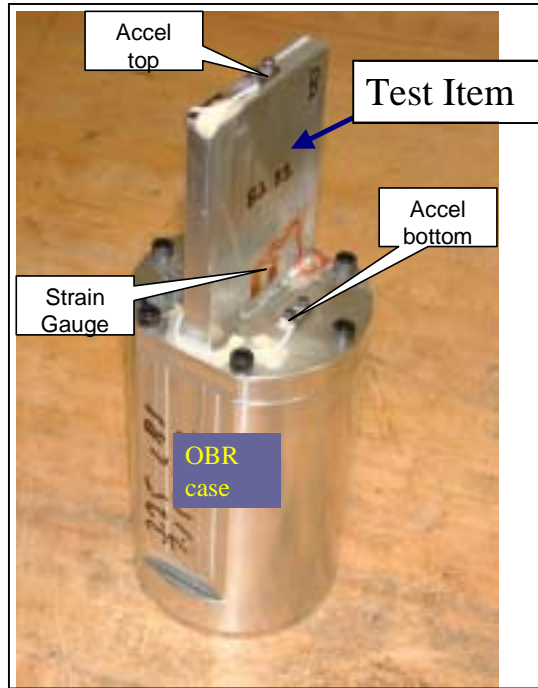


Figure 5. An instrumented test projectile.

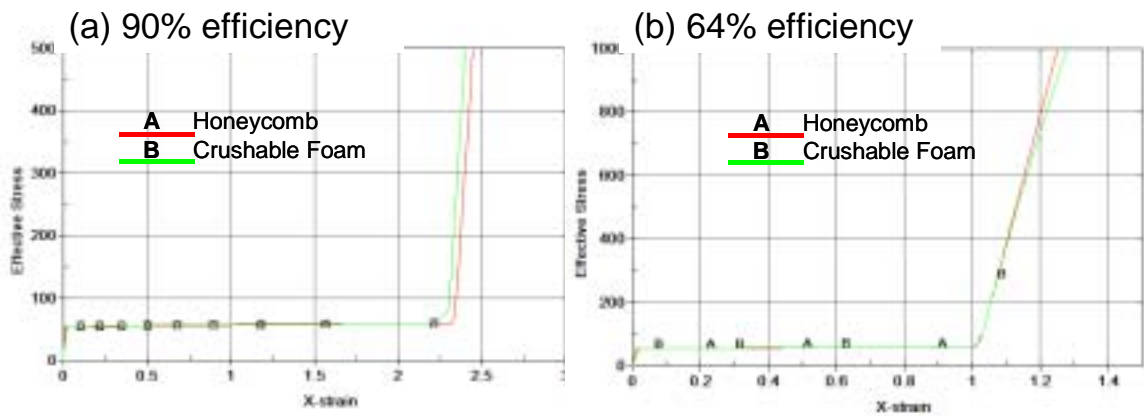
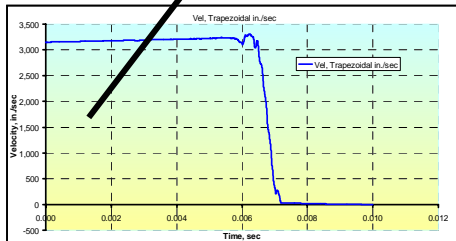
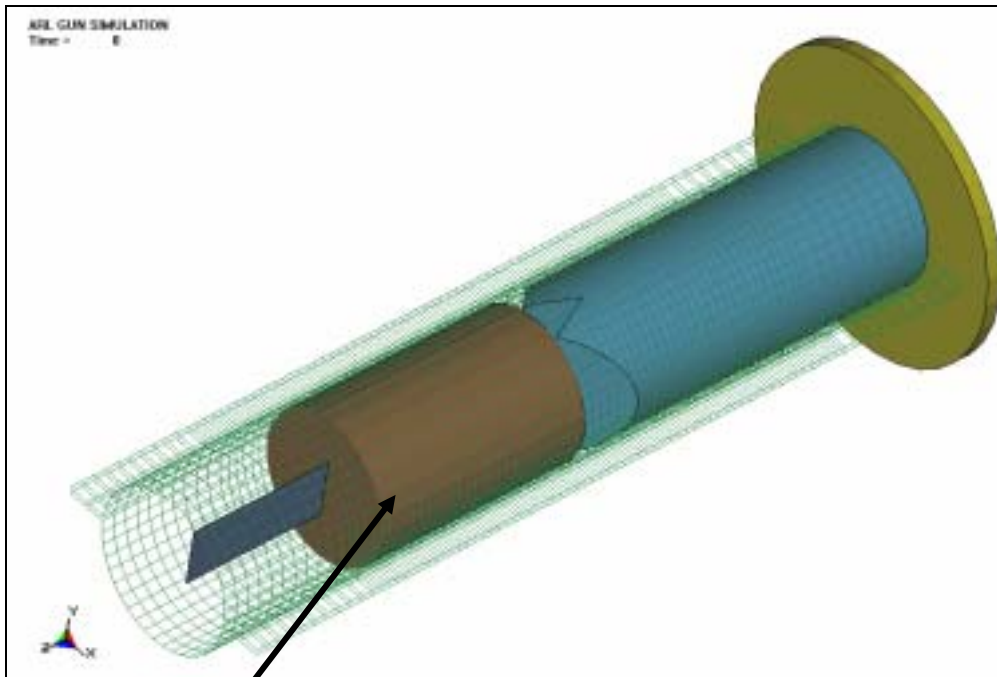


Figure 6. Simulated stress-strain curves using two materials models, 90% and 64% compaction (stress is in N/mm<sup>2</sup>).



Initial velocity for the OBR

Figure 7. The Lagrangian finite element mesh

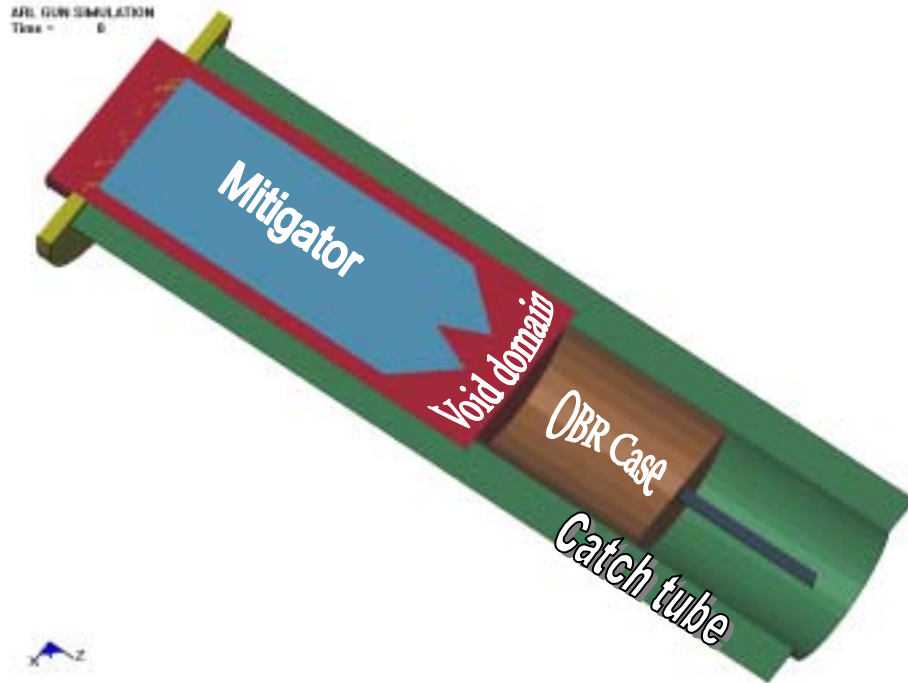


Figure 8. Section cut of ALE model.

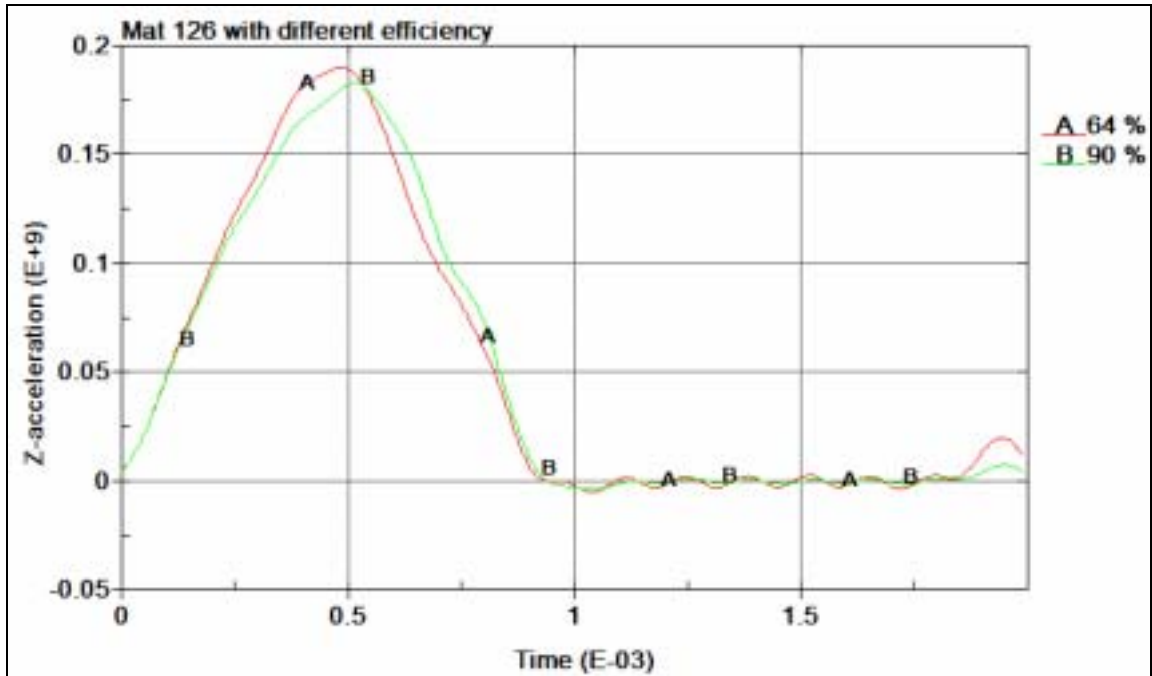


Figure 9. Acceleration of the top of the OBR for two different efficiencies.

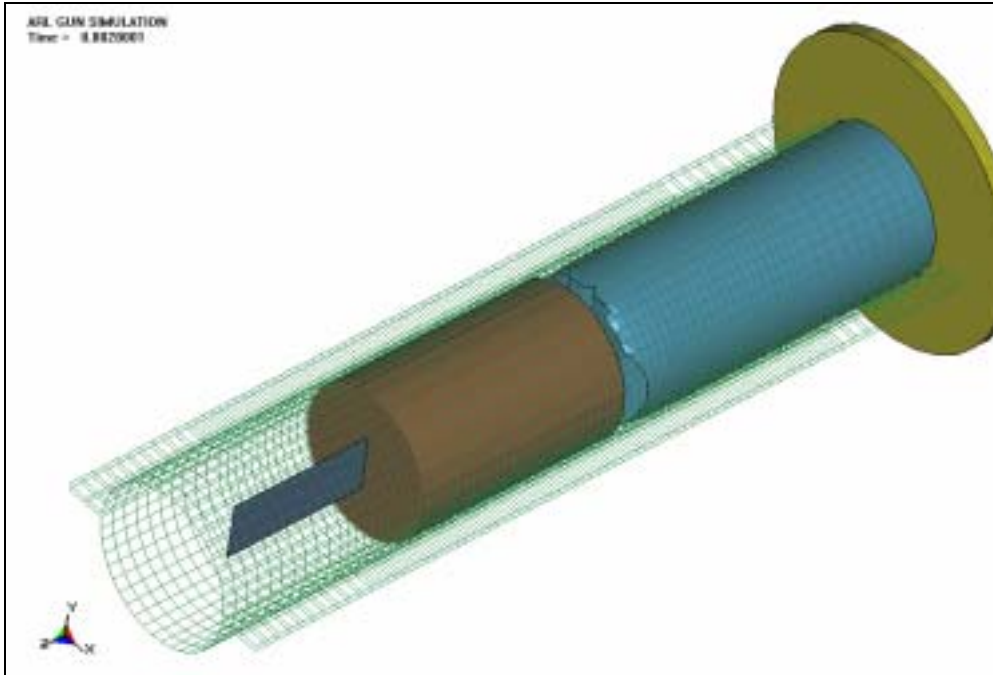


Figure 10. Impact simulation with the honeycomb material model.

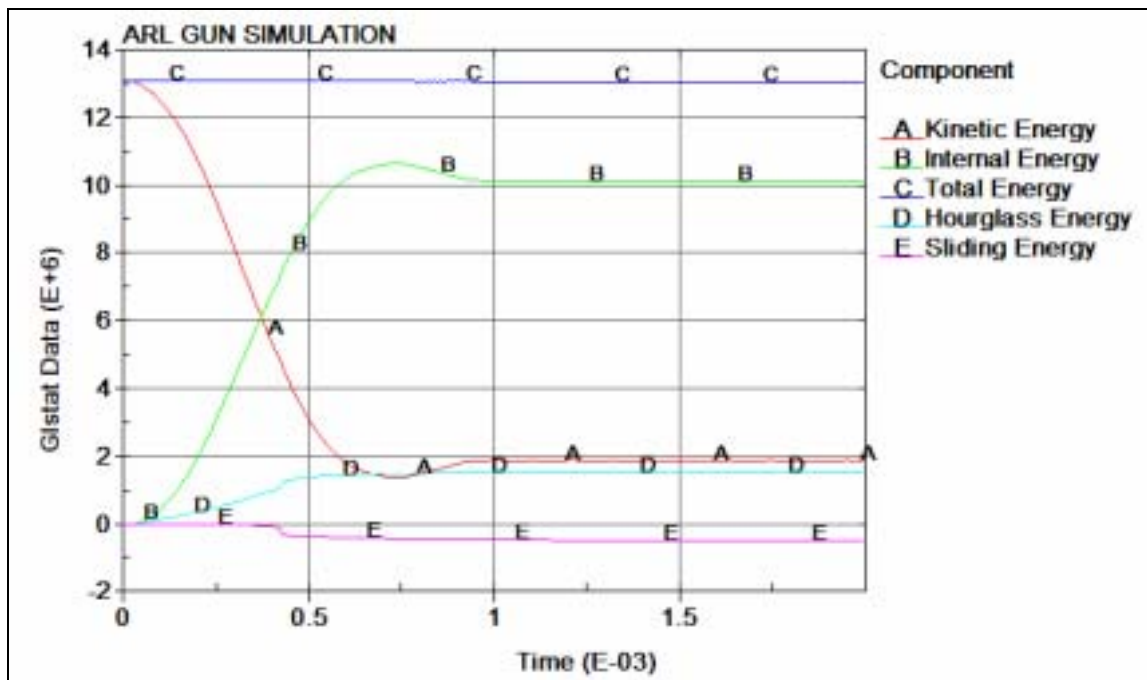


Figure 11. Energy balance, honeycomb material model.

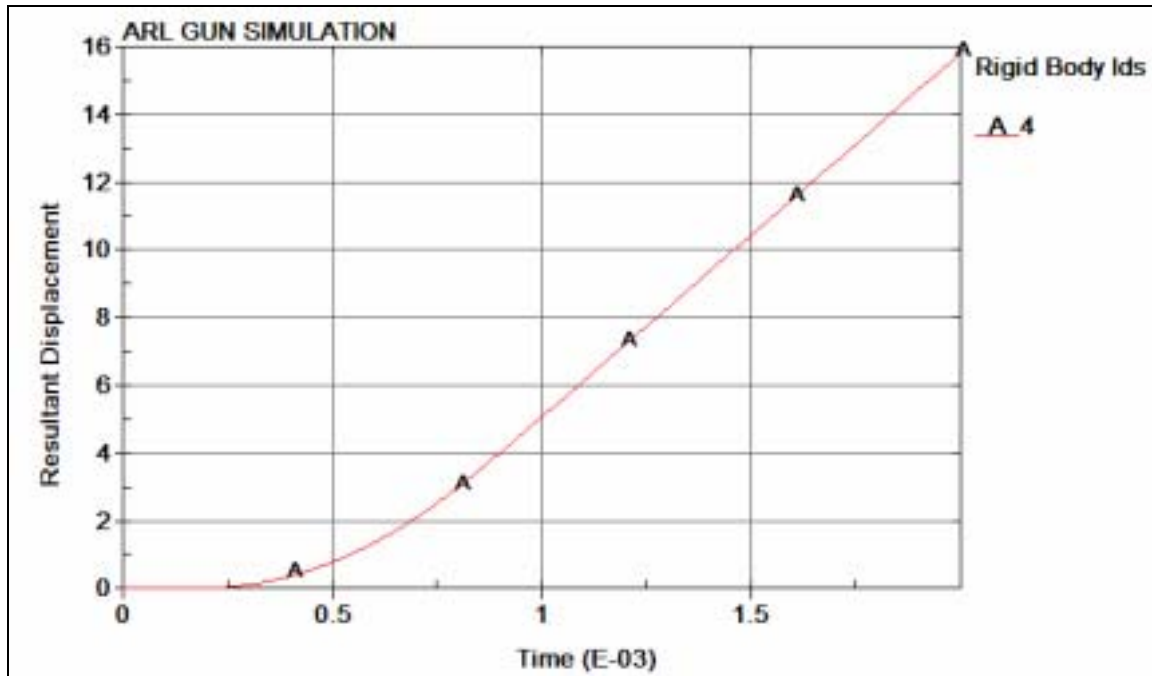


Figure 12. Displacement of the MEM, honeycomb material model.

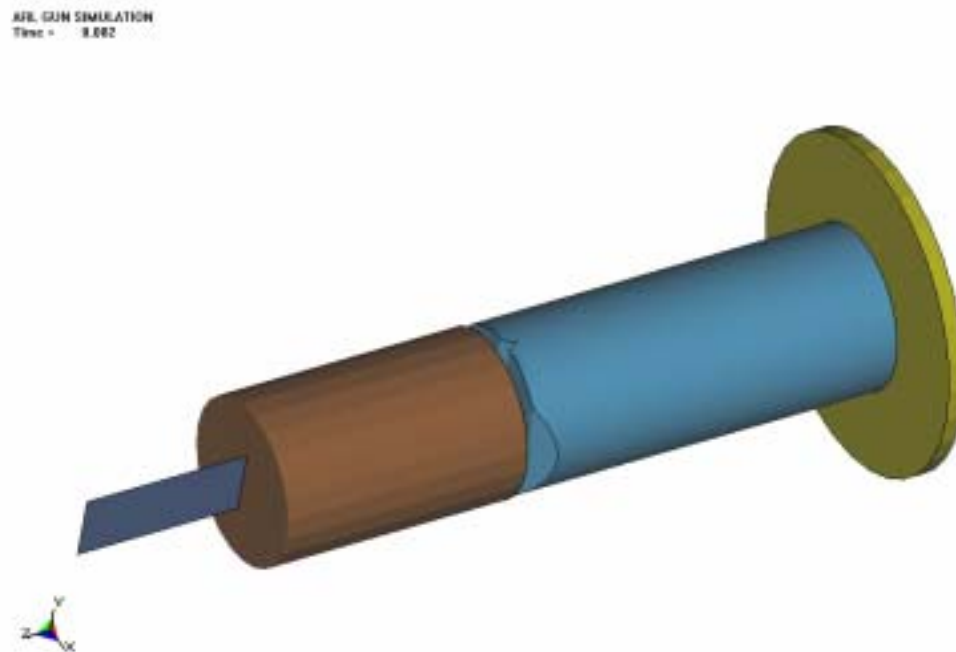


Figure 13. Crushed mitigator, crushable foam model.

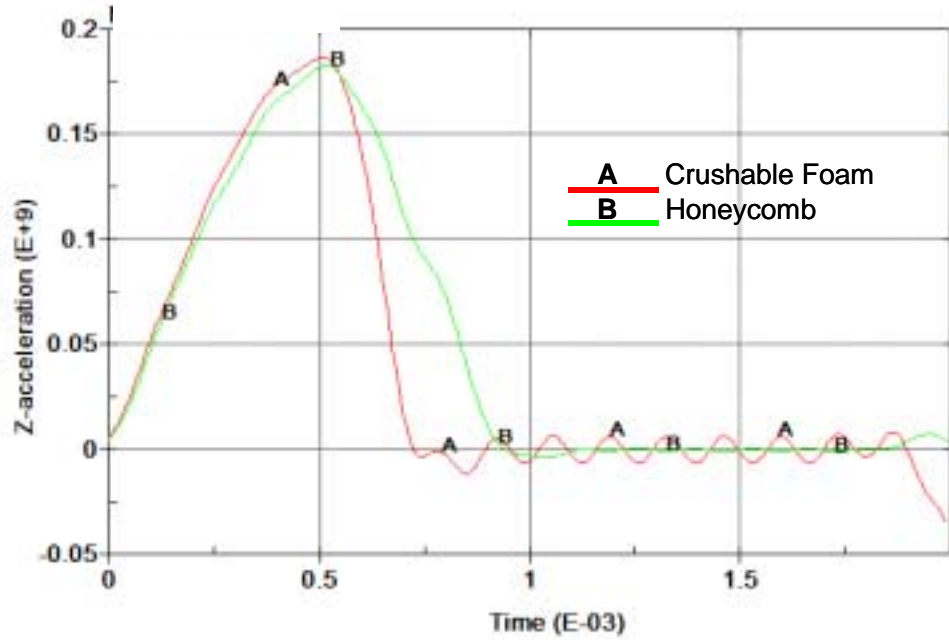


Figure 14. Acceleration (in mm per sec<sup>2</sup>) of the top of the OBR with honeycomb and crushable foam models.

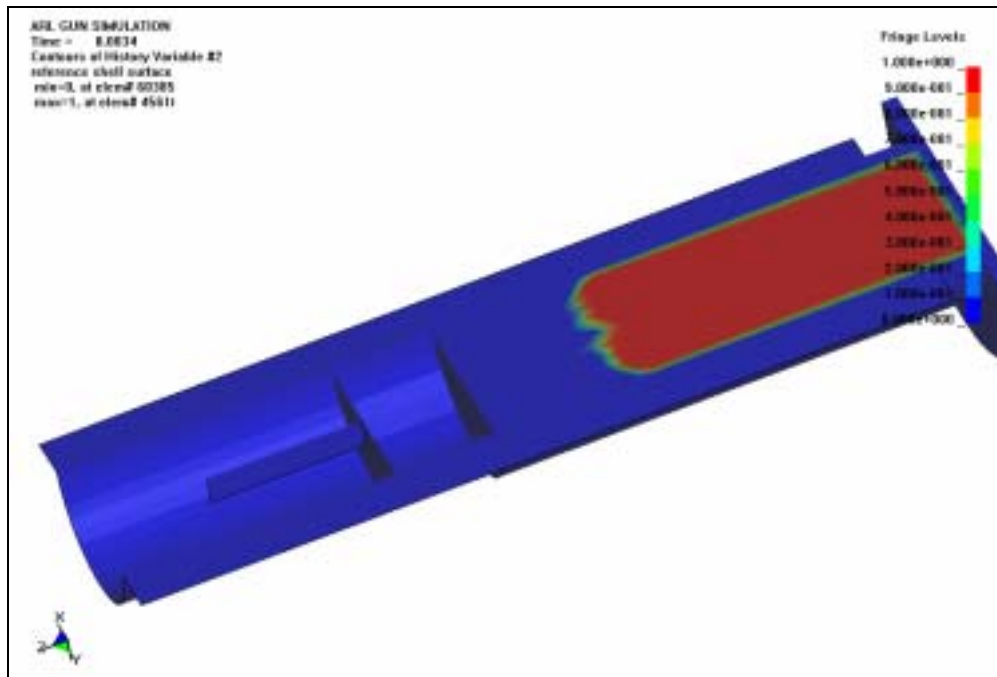


Figure 15. Volume fraction of the mitigator at the end of the simulation.

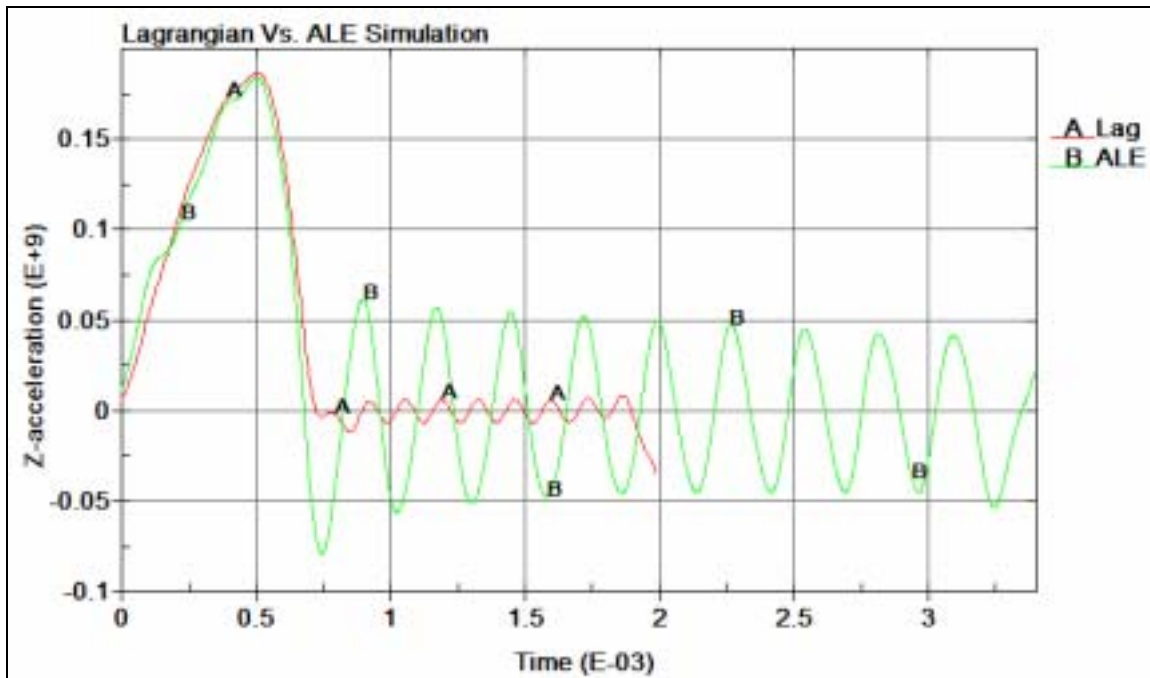


Figure 16. Acceleration (in  $\text{mm per sec}^2$ ) of the top of the OBR filtered at 2500 Hz for both the Lagrangian and ALE simulations.

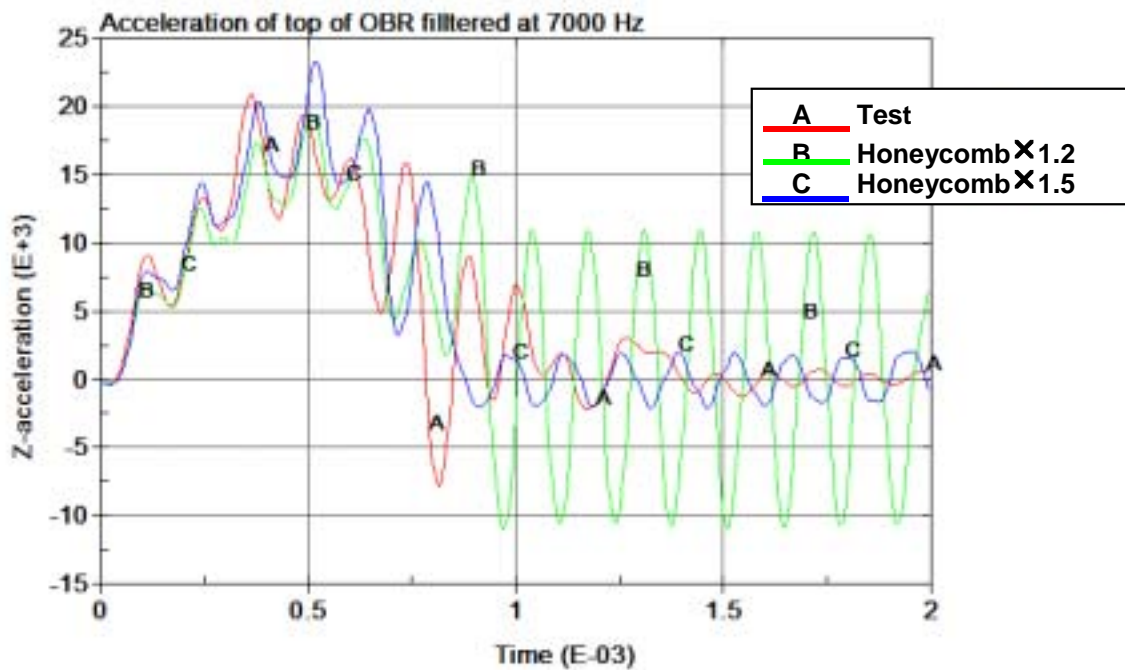
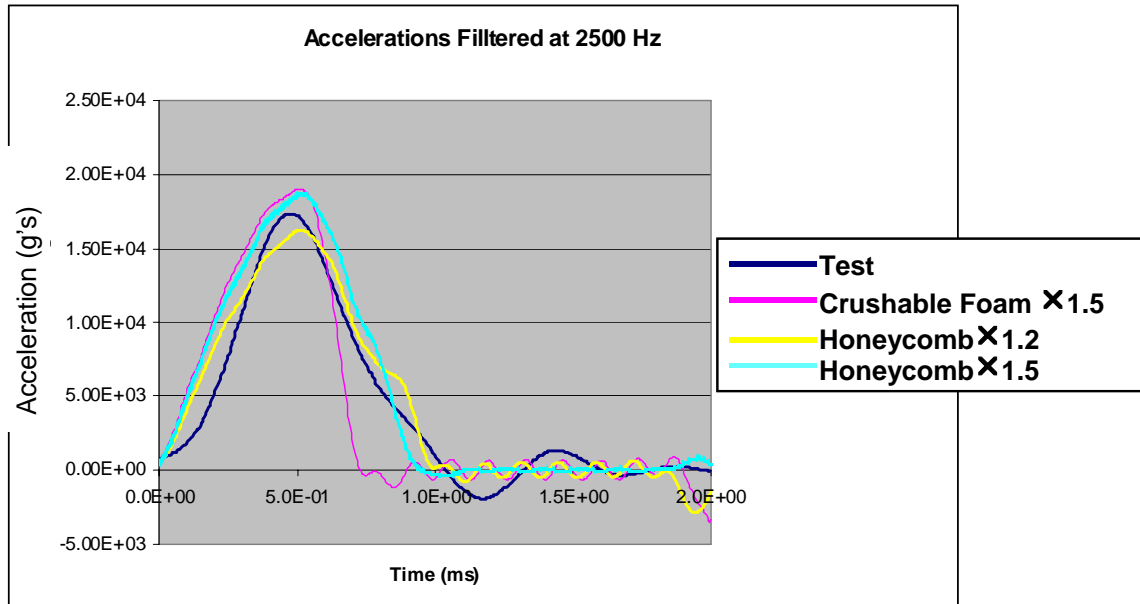


Figure 17. Simulation versus experiment, acceleration (in g's) of top of OBR filtered at 7000 Hz.



**Figure 18. Simulation versus experiment, acceleration of top of OBR filtered at 2500 Hz.**

- Figure 1. Schematic of an air gun test setup.
- Figure 2. A pre-shot arrangement in the 4-inch air gun test.
- Figure 3. A post-shot configuration of interacting components in a 4-inch air gun test.
- Figure 4. A post-shot view of an Al crushed mitigator.
- Figure 5. An instrumented test projectile.
- Figure 6. Simulated stress-strain curves using two materials models, 90% and 64% compaction (Stress is in  $\text{N}/\text{mm}^2$ ).
- Figure 7. The Lagrangian finite element mesh
- Figure 8. Section cut of ALE model.
- Figure 9. Acceleration of the top of the OBR for two different efficiencies.
- Figure 10. Impact simulation with the honeycomb material model.
- Figure 11. Energy balance, honeycomb material model.
- Figure 12. Displacement of the MEM, honeycomb material model.
- Figure 13. Crushed mitigator, crushable foam model.
- Figure 14. Acceleration (in  $\text{mm per sec}^2$ ) of the top of the OBR with honeycomb and crushable foam models.
- Figure 15. Volume fraction of the mitigator at the end of the simulation.
- Figure 16. Acceleration (in  $\text{mm per sec}^2$ ) of the top of the OBR filtered at 2500 Hz for both the Lagrangian and ALE simulations.
- Figure 17. Simulation versus experiment, acceleration ( $\text{g}'\text{s}$ ) of top of OBR filtered at 7000 Hz.
- Figure 18. Simulation versus experiment, acceleration of top of OBR filtered at 2500 Hz.